

Noncovalent Assembly of Targeted Carbon Nanovectors Enables Synergistic Drug and Radiation Cancer Therapy *in Vivo*

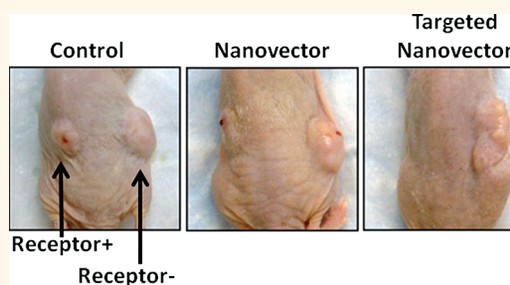
Daisuke Sano,^{†,*,||} Jacob M. Berlin,^{†,*,||} Tam T. Pham,^{†,||} Daniela C. Marcano,[†] David R. Valdecanas,[§] Ge Zhou,[†] Luka Milas,[§] Jeffrey N. Myers,^{†,*} and James M. Tour^{†,*}

[†]Department of Head and Neck Surgery, Unit 441, and the [§]Department of Experimental Radiation Oncology, Unit 1950, The University of Texas M. D. Anderson Cancer Center, 1515 Holcombe Boulevard, Houston, Texas 77030, United States and [†]Department of Chemistry and the Smalley Institute for Nanoscale Science and Technology, Rice University, MS-222, 6100 Main Street, Houston, Texas 77005, United States. [‡]Present address: Department of Biology and Function in Head and Neck, Yokohama City University Graduate School of Medicine, Yokohama, Japan (D.S.); Department of Molecular Medicine, The Beckman Research Institute of the City of Hope, Duarte, California (J.M.B.). ^{||}These authors contributed equally.

Head and neck squamous cell carcinoma (HNSCC) represents approximately 3.2% of cancers in the United States and accounted for approximately 49 260 new cancer diagnoses and 7600 deaths in 2010.¹ Despite advances in diagnosis and treatment, the 5-year survival of patients with HNSCC has not improved appreciably over the past few decades.² One reason for the high treatment failure rate is that the therapeutic ratios of chemotherapy and radiation therapy alone or in combination are not high enough and patients often relapse after these treatments and/or have significant treatment-related toxicities. Multimodal therapy that combines targeted drug delivery with radiation therapy and possibly surgical resection has shown promise to overcome this limitation and improve patient outcomes.³

There is a growing awareness that due to the heterogeneity of cancer, such an approach will demand personalized targeting components to realize its potential.^{4,5} Personalized medicine will involve the characterization of a patient's tumor(s), the identification of which drugs and targeting ligands will be effective, and finally the preparation of a final formulation that will use these ligands to deliver the drugs selectively to the cancer cells. One class of materials identified as potentially suitable platforms for the synergistic assembly of drugs and targeting ligands are nanovectors, which are materials with dimensions in the size range 1–100 nm that are capable of transporting and delivering one or more

ABSTRACT



Current chemotherapeutics are characterized by efficient tumor cell-killing and severe side effects mostly derived from off-target toxicity. Hence targeted delivery of these drugs to tumor cells is actively sought. In an *in vitro* system, we previously demonstrated that targeted drug delivery to cancer cells overexpressing epidermal growth factor receptor (EGFR+) can be achieved by poly(ethylene glycol)-functionalized carbon nanovectors simply mixed with a drug, paclitaxel, and an antibody that binds to the epidermal growth factor receptor, cetuximab. This construct is unusual in that all three components are assembled through noncovalent interactions. Here we show that this same construct is effective *in vivo*, enhancing radiotherapy of EGFR+ tumors. This targeted nanovector system has the potential to be a new therapy for head and neck squamous cell carcinomas, deserving of further preclinical development.

KEYWORDS: targeted drug delivery · cancer · nanovectors · hydrophilic carbon clusters · cetuximab · EGFR+

bioactive molecules.^{6,7} Nanovectors can carry multiple drugs, imaging agents, and targeting ligands, and drug-loaded nanovectors have demonstrated enhanced efficacy with reduced toxic side effects as compared to conventional systemic chemotherapies.^{8–11} However, for nanovectors to fully enable personalized medicine, the final assembly of drugs and targeting ligands must be simple

* Address correspondence to
jmyers@mdanderson.org;
tour@rice.edu.

Received for review December 13, 2011
and accepted February 8, 2012.

Published online February 08, 2012
10.1021/nn204885f

© 2012 American Chemical Society

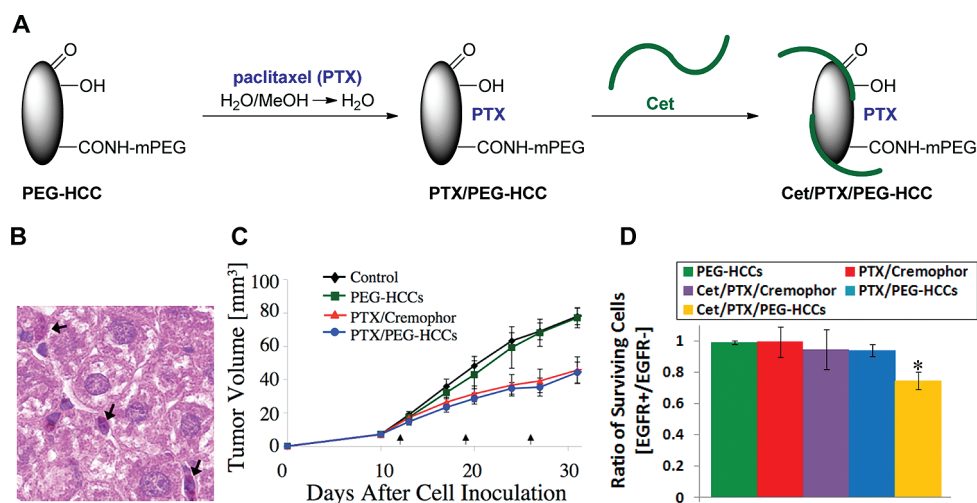


Figure 1. Development of Cet/PTX/PEG-HCCs. (A) PEG-HCCs have carbon cores approximately 40 nm × 1 nm functionalized with various oxygen-containing functional groups (note that only one each of several representative groups are shown). PEG is conjugated to the core *via* an amide bond. By simple mixing protocols, the PEG-HCCs can be loaded with PTX and wrapped with Cet. (B) Administering PEG-HCCs weekly to mice for 10 weeks results in no detectable toxicity, represented here by an image (100×) of the liver from a mouse treated for 10 weeks. The edge length of the image is 200 μm. The arrows mark the darker spots that likely indicate the presence of trace PEG-HCC aggregates. (C) PTX/PEG-HCCs have efficacy equivalent to Taxol (PTX/Cremophor) for treating a murine orthotopic model of head and neck cancer. The arrows indicate the time points of delivered treatment. (D) When PTX/PEG-HCCs are functionalized with Cet, they target the delivery of PTX to EGFR⁺ cells *in vitro*. **p* < 0.05.

and modular such that the final therapeutic can be prepared in a timely manner for the patient.

We have been working toward this goal by developing a nanovector that can be loaded with hydrophobic drugs and functionalized with targeting antibodies all by simple mixing. For a proof-of-principle demonstration, paclitaxel (PTX) was selected as the drug to be studied, as it is a classic example of a water-insoluble drug with high therapeutic efficacy and severe off-target toxicity. Cetuximab (Erbix, ImClone Systems) (Cet) is an IgG monoclonal antibody that exclusively binds to epidermal growth factor receptor (EGFR) with high affinity and blocks the normal function of the receptor.^{12–14} It was chosen as the targeting antibody because it is the most widely studied EGFR targeting agent and is approved by the Food and Drug Administration for the treatment of patients with HNSCC.^{15,16} Approximately 90% of HNSCCs overexpress the EGFR, and this is correlated with worse clinical outcomes.¹⁷

We previously reported on the preparation of extremely small (<40 nm long and 1 nm wide) hydrophilic carbon clusters (HCCs) that are poly(ethylene glycol) (PEG) functionalized (PEG-HCCs) (Figure 1).^{18–21} Preliminary studies suggested that the PEG-HCCs were not toxic.¹⁸ When the PEG-HCCs were administered to mice at a dose (1 g/L) of up to 10× that used for drug delivery, no acute toxicity was observed over 5 d. After 5 d the mice were euthanized, a terminal blood sample was collected, and the major organs including the heart, lungs, spleen, kidneys, liver, and brain were removed and examined for gross toxicity. At all tested concentrations, no abnormalities were seen in any of

the organs, warranting a longer term toxicity experiment. Thus, nude mice received a tail vein injection of PEG-HCCs (200 mg/L, 2× the drug delivery concentration) once per week, for up to 10 weeks. All animals were observed daily; the mice did not show any visual signs of fatigue or discomfort and slowly increased in body weight over the 10-week period. Mice were euthanized after 1, 2, 4, 6, 8, and 10 weeks of weekly treatments for histological analysis, and no gross toxicity was apparent in any of the organs analyzed. Total blood counts were performed on the mice, and all analytes were within normal ranges. Finally, biodistribution studies indicated that the PEG-HCCs had a blood half-life of 2 to 3 h; the large majority of the PEG-HCCs were excreted through the kidneys, the primary accumulation of the trace agglomerated carbon was in the liver and spleen, but no lesions were seen.¹⁸

We showed that PEG-HCCs are able to sequester PTX (collectively PTX/PEG-HCCs; in this nomenclature, the slash “/” signifies a noncovalent linkage and the hyphen “-” signifies a covalent bond) by physisorption and to deliver the drug for killing of cancer cells *in vitro* and *in vivo*.¹⁸ It was shown that the PTX/PEG-HCCs were stable in solution for at least 5 months. Both clinical formulations of PTX, Taxol and Abraxane, make use of a similar strategy of solubilizing unmodified PTX, likely due to both the ease of preparing this class of formulations and the fact that covalently modifying the PTX can alter its efficacy. Both *in vitro* and *in vivo*, the efficacy of PTX/PEG-HCCs was equivalent to that of Taxol (Bristol-Myers-Squibb, Princeton, NJ, USA), which is PTX solubilized in ethanol and a polyethoxylated castor oil, Cremophor EL (PTX/Cremophor). We further

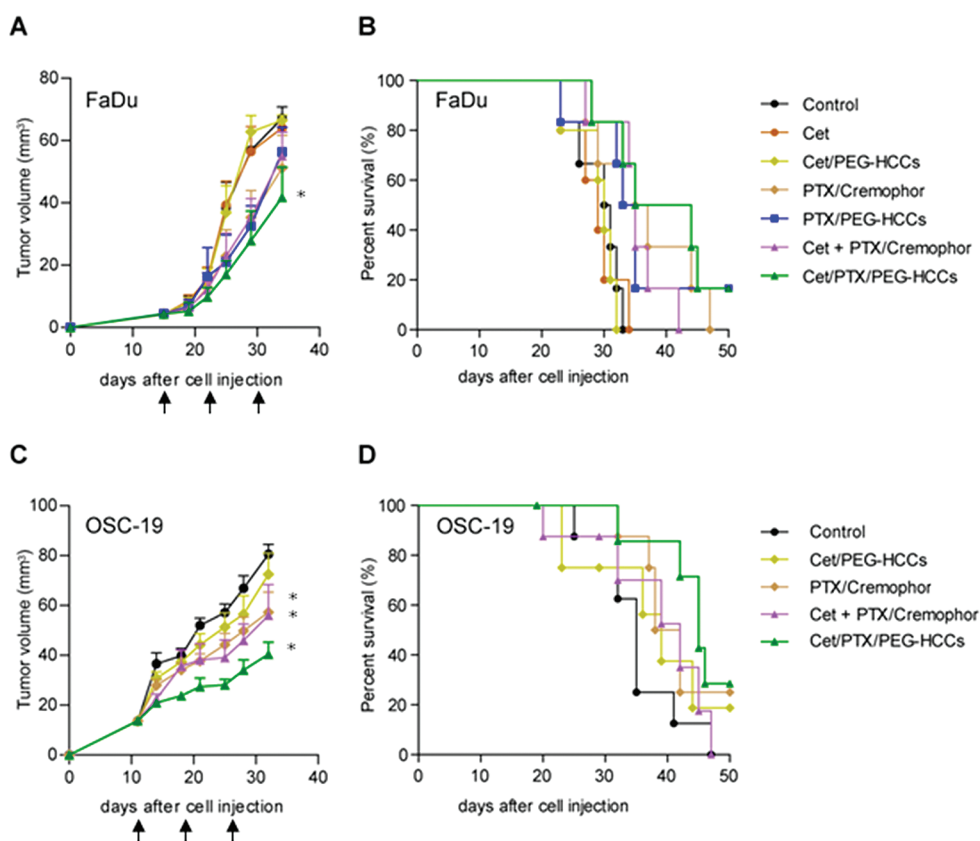


Figure 2. Treatment effect on tumor growth and survival for mice bearing tumors derived from FaDu cells (A, B) or OSC-19 cells (C, D). Plots A and C represent the tumor size, while B and D are the mouse survival plots. Mice with orthotopically established oral tongue tumors were injected *via* the tail vein once weekly (indicated with black arrows) with the treatment. Survival was analyzed by the Kaplan–Meier method and compared with log-rank tests. * $p < 0.05$ compared to the control at day 34.

showed that mixing the PTX/PEG-HCCs with Cet results in a targeted drug delivery vehicle (Cet/PTX/PEG-HCCs) in which both the drug and the antibody are physisorbed on the amphiphilic carbon core of the nanovectors. We demonstrated that Cet/PTX/PEG-HCCs is stable for >6 h in the presence of a physiological concentration of albumin and that it targets *in vitro* the delivery of PTX to EGFR+ cells *via* binding to the EGFR.²² Since the blood half-life of the PEG-HCCs is 3 h, we hypothesized that the Cet/PTX/PEG-HCCs might be stable during their period of circulation *in vivo*. Here we demonstrate that this readily prepared targeted drug delivery vehicle is effective *in vivo* and can be used to radiosensitize tumor cells in *in vitro* and *in vivo* models of human HNSCC.

RESULTS AND DISCUSSION

We began by comparing the efficacy of Cet/PTX/PEG-HCCs to Cet/PTX/Cremophor and the appropriate controls for the treatment of an orthotopic nude mouse model of tongue cancer derived from FaDu cells (Figure 2A,B). A very low amount of Cet (36 $\mu\text{g}/\text{mL}$) was used to prepare the Cet/PTX/PEG-HCCs. This amount of Cet alone or in combination with the PEG-HCCs did not show any antitumor effect. Consistent

with our previous results, PTX/Cremophor and PTX/PEG-HCCs showed an equivalent antitumor effect. Combining Cet with PTX/Cremophor did not increase the efficacy of the treatment, as this formulation was as effective as the two nontargeted formulations. However, in this tumor model, while these three treatments appear to be modestly effective, they are not statistically significantly different from the control group. The only treatment in this model that had a significantly enhanced antitumor effect relative to the control was the Cet/PTX/PEG-HCCs, but the efficacy of this treatment was not significantly different from that of any treatment containing PTX. The results from this particular cell line were suggestive but not conclusive.

Thus, we compared a smaller subset of the treatments in this same tumor model, but with tumors derived from OSC-19 cells (Figure 2C,D). Again, PTX/Cremophor and Cet/PTX/Cremophor showed equivalent efficacy, but, in this case, there was a significant delay in tumor growth and extension of survival. Cet/PTX/PEG-HCCs treatment also resulted in a significant delay in tumor growth and extension of survival, but while this treatment appeared to be more effective than either of the Cremophor-based treatments, that difference was not significant.

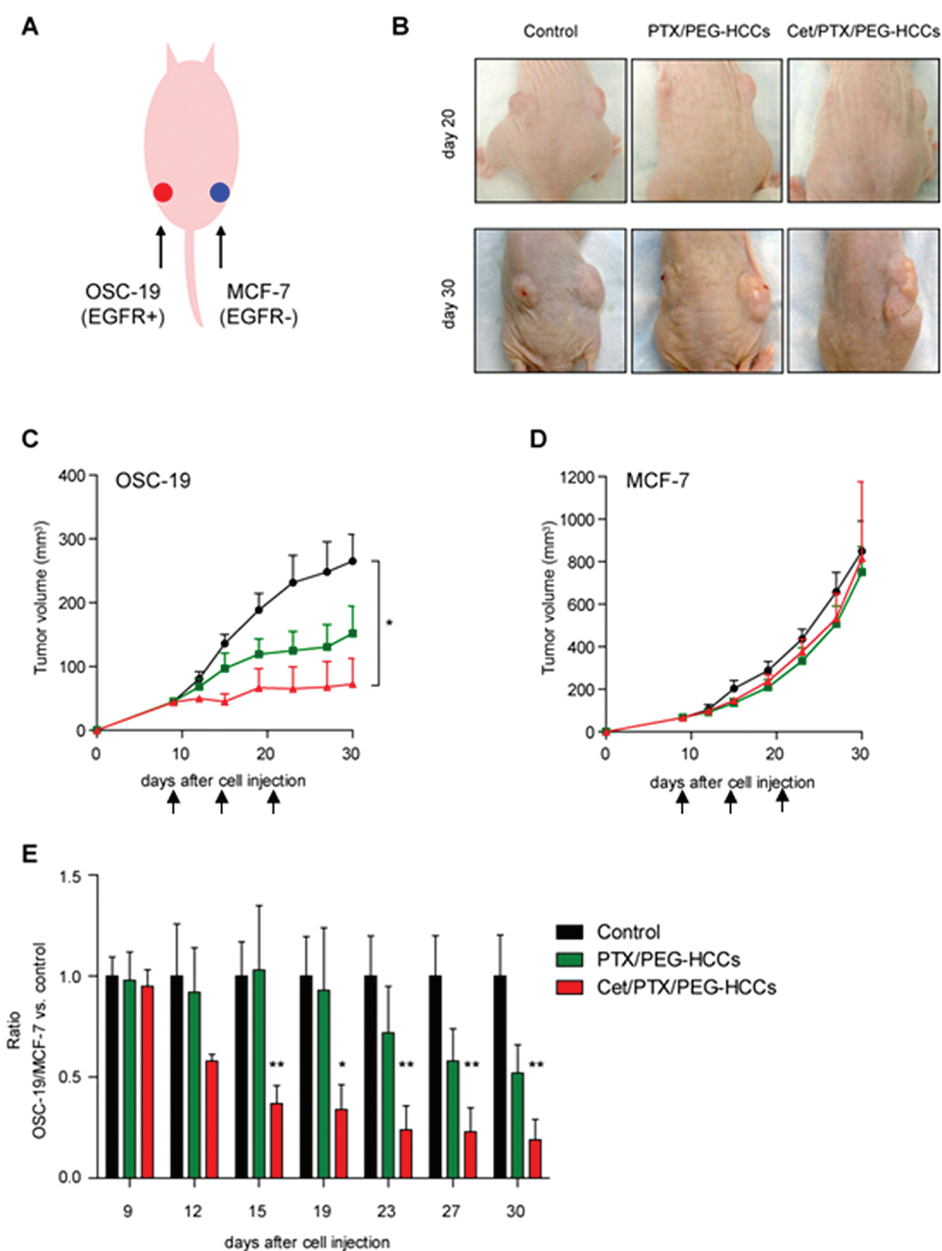


Figure 3. Effect of PTX/PEG-HCCs or Cet/PTX/PEG-HCCs on dual subcutaneous tumors in a nude mouse. (A) OSC-19 tumors (EGFR-positive; 1.5×10^6 cells per flank) were grown on the left flank and MCF-7 (EGFR-negative; 3×10^6 cells with Matrigel per flank) tumors on the right flanks of nude mice. (B) Effects of treatment on both OSC-19 and MCF-7 tumors. (C) Effect of treatment on OSC-19 tumors. Mice with established tumors were injected *via* the tail vein once weekly (indicated with black arrows) with the treatment. (D) Effect of treatment on MCF-7 tumors. Mice with established tumors were injected *via* the tail vein once weekly (indicated with black arrows) with the treatment. (E) Ratio was determined as the ratio for OSC-19 tumors/MCF-7 tumors divided by 1 in the control group. Points indicate means; bars, standard errors. * $p < 0.05$; ** $p < 0.01$.

In order to better understand if the Cet/PTX/PEG-HCCs were targeting the delivery of PTX to EGFR-positive tumor cells, we used a dual subcutaneous tumor model with OSC-19 (EGFR positive) and MCF-7 (EGFR negative) tumor cells injected on the opposing flanks of nude mice. These mice were then systemically treated with either saline, PTX/PEG-HCCs, or Cet/PTX/PEG-HCCs (Figure 3). The EGFR-positive tumor showed a markedly enhanced response to treatment with the targeted formulation (Figure 3C); however, the EGFR-negative tumor showed no difference in response

when treated with either the PTX/PEG-HCCs or the Cet/PTX/PEG-HCCs (Figure 3D). While it is possible that the difference in conditions necessary to establish the two tumors, including the use of Matrigel for the MCF-7 cells, and/or physiological differences between the two tumors might have contributed to the different responses to treatment, the dominant effect could indeed be due to the targeted delivery of PTX to the EGFR-positive tumor by the Cet/PTX/PEG-HCCs. Even though Cet/PTX/PEG-HCCs appear to target the delivery of PTX to EGFR-positive tumor cells, the

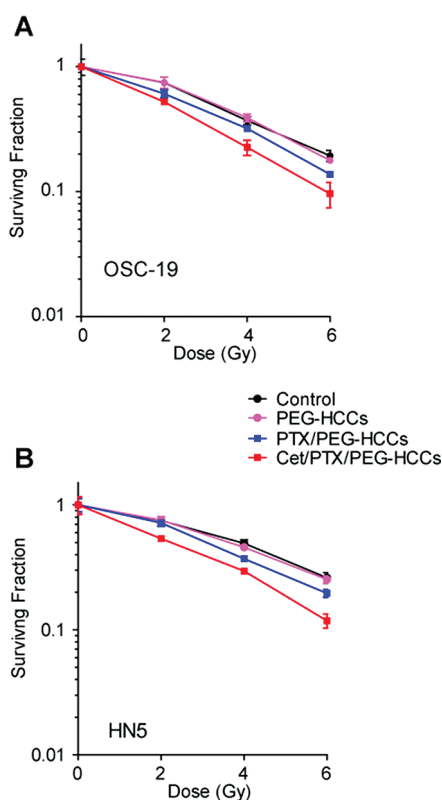


Figure 4. Effects of PTX/PEG-HCCs or Cet/PTX/PEG-HCCs on head and neck squamous cell carcinoma cells' radiosensitivity. (A) Effect of treatment on OSC19 cells. (B) Effect of treatment on HN5 cells. OSC-19 and HN5 cells in culture were exposed to PEG-HCCs (0.96 $\mu\text{g}/\text{mL}$), PTX/PEG-HCCs (PTX 4 nM, PEG-HCCs 0.96 $\mu\text{g}/\text{mL}$), or Cet/PTX/PEG-HCCs (Cet 0.8 pM, PTX 4 nM, PEG-HCCs 0.96 $\mu\text{g}/\text{mL}$) for 1 h and then irradiated at 2, 4, or 6 Gy. After treatments, clonogenic survival assays were performed. Points indicate the means of triplicate experiments; bars, standard errors.

improvement over PTX/PEG-HCCs is modest. In tumor models where the efficacy of PTX/PEG-HCCs itself is limited, Cet/PTX/PEG-HCCs and PTX/PEG-HCCs might show no significant difference. Thus, radiation treatment was combined with nanovector treatment both because the boost in efficacy from radiation treatment would allow us to confirm a difference in activity for the two treatments and because it models a clinically relevant treatment mode.

It is known that Cet and PTX each enhance the radiation response of HNSCC.²³ In fact, inhibiting the EGFR pathway has been reported to enhance radiosensitization in both preclinical and clinical study.^{16,24} Since the use of the Cet/PTX/PEG-HCCs appears to result in the co-localization of Cet and PTX, the radiosensitizing property of this therapy was evaluated. To assess whether Cet/PTX/PEG-HCCs could sensitize HNSCC cells to radiation therapy *in vitro*, OSC-19 and HN5 cells were treated with saline, Cet, PEG-HCCs, PTX/Cremophor, PTX/PEG-HCCs, or Cet/PTX/PEG-HCCs and then exposed to radiation (Figure 4). The effects on the cells were assessed with clonogenic survival assays. In these assays, radiation alone resulted in a

dose-dependent decrease in OSC-19 and HN5 cell survival. These results are very similar to our previous report.²⁵ Both PEG-HCCs and Cet did not show any additional cell growth inhibition compared to control (radiation alone treatment). Treatment with either PTX/Cremophor (data not shown) or PTX/PEG-HCCs resulted in an identical and significant enhancement in cell growth inhibition, and cells treated with Cet/PTX/PEG-HCCs exhibited the greatest enhancement in growth inhibition.

Encouraged by the *in vitro* results, we evaluated treating nude mice bearing an orthotopic tumor with radiotherapy (RT) alone or in combination with PEG-HCCs combined with PTX or Cet/PTX. As in Figure 4, we evaluated tumors derived from two different HNSCC cell lines, OSC-19 and HN5. In the OSC-19-luc model, there was a significant antitumor effect on day 20 after cell inoculation in the mice treated with Cet/PTX/PEG-HCCs + RT compared with the mice in the control group ($p < 0.0001$; Figure 5A). Moreover, while several of the other treatments resulted in significant tumor growth delay relative to the control group, the tumor growth delay produced by treatment with Cet/PTX/PEG-HCCs + RT was statistically significant when compared to each of the other treatment groups (vs PTX/PEG-HCCs $p < 0.0001$, Cet/PTX/PEG-HCCs $p = 0.0136$, RT $p = 0.0114$, and PTX/PEG-HCCs + RT $p = 0.0041$, respectively). Treatment with Cet/PTX/PEG-HCCs + RT also resulted in the greatest increase in survival time (Figure 5B).

The antitumor effects of combining the PTX treatments with RT were also evaluated in an orthotopic model derived from a different cell line, HN5 (Figure 5C). Similar results were obtained, as the mice treated with Cet/PTX/PEG-HCCs + RT had a significantly lower mean tumor volume than the mice in the control group at day 27 ($p = 0.0002$). In addition, the mice treated with Cet/PTX/PEG-HCCs + RT had a significantly lower mean tumor volume than the mice in the PTX/PEG-HCCs alone group, Cet/PTX/PEG-HCCs alone group, and the RT alone group ($p = 0.0013$, $p = 0.0351$, and $p = 0.0335$, respectively). Treatment with Cet/PTX/PEG-HCCs + RT also resulted in the greatest increase in survival time (Figure 5D). Finally, for both OSC-19-luc and HN5 cells, all treatments appeared to be well-tolerated, with no evidence of treatment-related weight loss (data not shown), and the experiments were repeated one additional time with similar results (data not shown).

In order to quantify the radiosensitization imparted by Cet/PTX/PEG-HCCs, the degree of growth delay observed for the OSC-19-luc model was expressed as the absolute tumor growth delay (AGD), defined as the average time in days required for the average tumor size in mice given a treatment to grow to 40 mm³ minus the time in days for the average tumor size in the untreated control group to reach the same size, or the

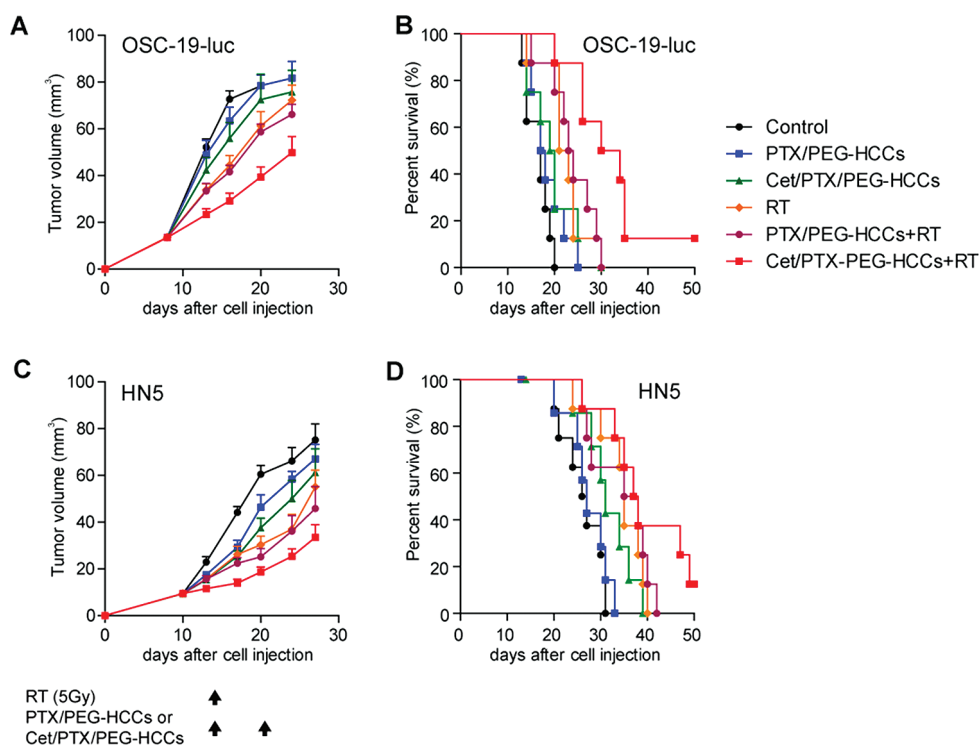


Figure 5. *In vivo* effects of treatment with radiation, PTX/PEG-HCCs, Cet/PTX/PEG-HCCs, and their combinations on tumor growth and survival time in mice. (A) *In vivo* effects of treatments on tumor growth in OSC-19-luc mice. Points indicate means; bars, standard errors (SE). (B) *In vivo* effects of treatments on survival time of OSC-19-luc mice. (C) *In vivo* effects of treatments on tumor growth in HN5 mice. Black arrows indicate treatment days. Points, mean; bars, SE (D) *In vivo* effects of treatments on survival time in HN5 mice. Animals were euthanized when they had lost more than 20% of their initial body weight or at 50 days after cell inoculation. Survival was analyzed by the Kaplan–Meier method and compared with log-rank tests.

TABLE 1. Effect of Treatment on OSC-19-luc Human Head and Neck Squamous Cell Carcinoma Cells' Radioresponse^a

treatment	time required to grow to 40 mm ³ , d	absolute growth delay, d	normalized growth delay, d	enhancement factor
control	13.5 ± 0.3			
PTX/PEG-HCCs	14.7 ± 0.8	1.2 ± 0.8		
Cet/PTX/PEG-HCCs	16.0 ± 1.7	2.5 ± 1.7		
RT	17.6 ± 1.1	4.1 ± 1.1		
PTX/PEG-HCCs+RT	17.4 ± 0.7	3.9 ± 0.7	2.8 ± 0.7	0.68
Cet/PTX/PEG-HCCs+RT ^b	21.9 ± 1.0	8.4 ± 1.0	5.9 ± 1.0	1.44

^a All data are means ± standard error. ^b One of 8 mice whose tumor volume never reached 40 mm³ was not used in the analysis.

normalized growth delay (NGD), defined as the time in days for the average tumor size to reach 40 mm³ in the mice treated with the combination of PTX/PEG-HCCs or Cet/PTX/PEG-HCCs plus radiation, minus the time in days to reach 40 mm³ in mice treated with PTX/PEG-HCCs or Cet/PTX/PEG-HCCs alone. Treatment enhancement factors (EFs) were obtained by dividing the NGD in mice treated with drugs plus radiation by the AGD in mice treated with radiation alone (Table 1).²⁶

Cet/PTX/PEG-HCCs + RT achieved a more than additive effect, resulting in an AGD of 8.4 ± 1.0 d, which was considerably higher than the sum of tumor growth delays caused by individual treatments (2.5 ± 1.7 d with Cet/PTX/PEG-HCCs alone and 4.1 ± 1.1 d with RT alone; EF = 1.44) even though one of eight mice whose tumor never reached 40 mm³ was not used in the analysis. Similarly, while PTX/PEG-HCCs did not

enhance the effect of RT in HN5 tumors (EF = 1.00), Cet/PTX/PEG-HCCs enhanced the radioresponsiveness of HN5 tumors, increasing tumor growth delay more than additively even though one of eight mice whose tumor never reached 40 mm³ was not used in the analysis (EF = 1.09/data not shown). Thus, Cet/PTX/PEG-HCCs enhanced HNSCC tumors' radioresponse.

CONCLUSION

Cet/PTX/PEG-HCCs, produced by simply mixing PTX/PEG-HCCs with Cet, appear to target tumors overexpressing EGFR *in vivo*. While the increase in efficacy relative to current clinical therapies is limited, when the therapies are combined with radiation, the Cet/PTX/PEG-HCCs are significantly more effective than the mixture of Cet and PTX/Cremophor. The increased efficacy of the targeted formulation might be due to

a synergy between inhibition of the EGFR pathway and the taxane effect.²⁷ Given the fact that most HNSCC patients receive multimodal therapy including radiation, the increased efficacy observed for Cet/PTX/PEG-

HCCs is particularly important. Future studies will be required to optimize the formulation and treatment protocol for maximal radiosensitization prior to translation toward the clinic.

MATERIALS AND METHODS

Animals. We purchased 8-to-12-week-old male athymic nude mice from the National Cancer Institute (Bethesda, MD, USA). The mice were kept in a specific pathogen-free facility approved by the American Association for the Accreditation of Laboratory Animal Care that met all current regulations and standards of the U.S. Department of Agriculture, U.S. Department of Health and Human Services, and the National Institutes of Health. Mice were fed irradiated standard mouse chow and autoclaved, reverse-osmosis-treated water. Animal procedures were carried out according to a protocol approved by The University of Texas MD Anderson Cancer Center's Institutional Animal Care and Use Committee.

Cell Lines. FaDu cells were purchased from American Type Culture Collection (Manassas, VA, USA). HN5 cells were provided by Dr. Zhen Fan (Department of Experimental Therapeutics, MD Anderson Cancer Center). OSC-19 was purchased from the Health Science Research Resources Bank (Osaka, Japan). MCF-7 cells were provided by Dr. Francois-Xavier Claret (Department of Systems Biology, MD Anderson Cancer Center). OSC-19 cells were retrovirally infected with the green fluorescent protein and the luciferase gene (OSC-19-luc) as described previously.²⁸ All cells were maintained in Dulbecco's modified Eagle's medium (DMEM) supplemented with 10% fetal bovine serum, L-glutamine, sodium pyruvate, nonessential amino acids, and a 2-fold vitamin solution (Life Technologies, Inc., Grand Island, NY, USA). Adherent monolayer cultures were maintained on plastic plates and incubated at 37 °C in 5% carbon dioxide and 95% oxygen. The integrity of all maintained cell lines was clearly established using short tandem repeat genomic profiling. The cultures were *Mycoplasma*-free and maintained for no longer than 12 weeks after they were recovered from frozen stocks.

Reagents. Hydrophilic carbon clusters that are covalently modified with polyethylene glycol (PEG-HCCs) were synthesized, and PEG-HCCs were loaded with paclitaxel (PTX/PEG-HCCs) as described previously.¹⁸ As we have done in all past publications,^{18,22} all concentrations given in this article for the PEG-HCCs are for the carbon cores of the PEG-HCCs, as this can be directly measured by ultraviolet–visible (UV–vis) spectroscopy. Cet (C225/Erbix; Imclone, New York, NY, USA), an anti-EGFR monoclonal antibody, is used as the targeting agent to establish Cet/PTX/PEG-HCCs and is attached by simply mixing it with PTX/PEG-HCCs. Paclitaxel (Taxol/Bristol-Myers Squibb, Princeton, NJ, USA) was diluted in PBS to a 982 µg/mL final concentration and Cet was also diluted in phosphate-buffered saline (PBS) to a 35.9 µg/mL final concentration for *in vivo* experiments.

Orthotopic Nude Mouse Model of HNSCC. To evaluate the effect of Cet/PTX/PEG-HCCs *in vivo*, we used an orthotopic nude mouse model of HNSCC because its host microenvironment is more similar to that of patients with HNSCC than that of subcutaneous xenograft models of HNSCC.²⁹ An orthotopic nude mouse model of oral tongue cancer was established by injecting FaDu (2.5×10^5) or OSC-19 (5×10^4) cells suspended in 30 µL of serum-free DMEM into the tongues of mice as described previously.³⁰

Twelve to 15 d after the cells were injected, the mice were randomly assigned to one of six or eight treatment groups (6 to 8 mice per group): (1) control; (2) PEG-HCCs (100 µg/mL); (3) Cet (35.9 µg/mL); (4) Cet/PEG-HCCs (Cet 35.9 µg/mL, PEG-HCCs 100 µg/mL); (5) PTX/Cremophor (982 µg/mL); (6) PTX/PEG-HCCs (PTX 982 µg/mL, PEG-HCCs 100 µg/mL); (7) Cet/PTX/Cremophor (Cet 35.9 µg/mL, PTX 982 µg/mL); (8) Cet/PTX/PEG-HCCs (Cet 35.9 µg/mL, PTX 982 µg/mL, PEG-HCCs 100 µg/mL). A dose of

200 µL of each treatment was administered intravenously once a week for 3 weeks. Control mice were given 200 µL of PBS intravenously once weekly for 3 weeks.

Mice were examined twice a week for tumor size and weight loss. Tongue tumor size was measured with microcalipers. Tumor volume was calculated as $(A)(B^2)\pi/6$, where A is the longest dimension of the tumor and B is the dimension of the tumor perpendicular to A . We euthanized mice by CO₂ asphyxiation when they lost more than 20% of their preinjection body weight or at 50 d after cell injection.

Dual Subcutaneous Tumors Model in a Nude Mouse. To confirm that Cet/PTX/PEG-HCCs target EGFR-positive cells *in vivo*, a dual subcutaneous tumor model was established in a nude mouse. As shown in Figure 1A, OSC-19 cells (EGFR-positive; 1.5×10^5) resuspended in PBS and MCF-7 cells (EGFR-negative; 3×10^5) resuspended in 50% Matrigel (BD Bioscience, Bedford, MA, USA) were injected subcutaneously in the left and right flank, respectively, as described previously.³¹ Nine days after implantation of cells, when the average OSC-19 tumor volume reached 44 mm³ and the average MCF-7 tumor volume reached 65 mm³, the mice were randomly assigned to one of three treatment groups (8 mice per group): control, PTX/PEG-HCCs, or Cet/PTX/PEG-HCCs. PTX/PEG-HCCs and Cet/PTX/PEG-HCCs were administered intravenously an injection of 200 µL once a week for 3 weeks. Control mice were given 200 µL of PBS intravenously once weekly for 3 weeks. Tumor sizes for both tumors were measured twice a week. The ratio of OSC-19/MCF-7 was also calculated for each time point as

$$\frac{(\text{OSC-19 tumor vol w/treatment}/\text{OSC-19 tumor vol w/o treatment})}{(\text{MCF-7 tumor vol w/treatment}/\text{MCF-7 tumor vol w/o treatment})}$$

Clonogenic Survival Assay. OSC-19 and HN5 cells were used, since they are radiation-resistant.²⁵ OSC-19 and HN5 cells in culture were exposed to PEG-HCCs (96 µg/mL), Cet (0.8 pM), PTX/Cremophor (4 nM), PTX/PEG-HCCs (PTX 4 nM, PEG-HCCs 96 µg/mL), or Cet/PTX/PEG-HCCs (Cet 0.8 pM, PTX 4 nM, PEG-HCCs 96 µg/mL) for 1 h and then exposed to 2, 4, or 6 Gy radiation (γ -rays using a cesium-137 source, 3.055 Gy/min). The cells were then assayed for colony-forming ability by trypsinizing and replating in 100 mm dishes in drug-free medium. After 10–11 d of incubation, the cells were stained with 0.5% crystal violet in absolute ethanol, and colonies with more than 50 cells were counted under a dissection microscope. Plating efficiency was defined as the percentage of cells seeded that grew into colonies under a specific culture condition of a given cell line. The survival fraction, expressed as a function of irradiation, was calculated as the number of colonies counted/(the number of cells seeded \times plating efficiency/100) as described previously.²⁵

Enhancement of Tumor Radioresponse by Cet/PTX/PEG-HCCs in an Orthotopic Nude Mouse Model of HNSCC. An orthotopic nude mouse model of oral cancer was established by injecting OSC-19-luc (1×10^5) or HN5 (3×10^5) cells suspended in 30 µL of serum-free DMEM into the tongues of mice as described.

Eight to 10 d after the cells were injected, the mice were randomly assigned to one of six treatment groups (7 or 8 mice per group): (1) control; (2) PTX/PEG-HCCs (PTX 982 µg/mL, PEG-HCCs 100 µg/mL); (3) Cet/PTX/PEG-HCCs (Cet 35.9 µg/mL, PTX 982 µg/mL, PEG-HCCs 100 µg/mL); (4) radiation; (5) radiation plus PTX/PEG-HCCs (PTX 982 µg/mL, PEG-HCCs 100 µg/mL); (6) radiation plus Cet/PTX/PEG-HCCs (Cet 35.9 µg/mL, PTX 982 µg/mL, PEG-HCCs 100 µg/mL). All drugs were administered intravenously at 200 µL once a week for 2 weeks. Control mice were given 200 µL of PBS intravenously once weekly for 2 weeks. Mice bearing tumors in the tongue were locally irradiated with a

single dose of 5 Gy using a small-animal irradiator (γ -rays using a cesium-137 source, 4.762 Gy/min). Sodium pentobarbital was administered by intraperitoneal injection at a dose of 50 mg/kg prior to radiation treatment. The mice were immobilized on a customized jig during irradiation with the tumor centered in the 3 cm diameter circular irradiation field as described previously.²⁵ When Cet/PTX/PEG-HCCs or PTX/PEG-HCCs and radiation were combined, drugs were given 1 h before single-dose irradiation.

Mice were examined twice a week for tumor size and weight loss. Tongue tumor size was measured with microcalipers as described above. The degree of growth delay was expressed as the absolute tumor growth delay, defined as the average time in days required for the average tumor size in mice given a treatment to grow to 40 mm³ minus the time in days for the average tumor size in the untreated control group to reach the same size, or the normalized growth delay, defined as the time in days for the average tumor size to reach 40 mm³ in the mice treated with the combination of PTX/PEG-HCCs or Cet/PTX/PEG-HCCs plus radiation, minus the time in days to reach 40 mm³ in mice treated with PTX/PEG-HCCs or Cet/PTX/PEG-HCCs alone. Treatment enhancement factors were obtained by dividing the NGD in mice treated with drugs plus radiation by the AGD in mice treated with radiation alone.²³ Mice were euthanized by CO₂ asphyxiation when they lost more than 20% of their preinjection body weight or at 50 d after cell injection.

Statistical Analysis. Two-tailed *t* tests were used to compare tumor volumes from control groups and treatment groups. Survival was determined using the Kaplan–Meier method and compared using log-rank tests. Statistical analyses were performed with Prism 5.01 software (GraphPad Software). *p* values < 0.05 were considered statistically significant.

Conflict of Interest: The authors declare no competing financial interest.

Acknowledgment. We thank the Alliance for NanoHealth through a subcontract from the University of Texas Health Science Center, Houston (Department of Defense: W8XWH-07-2-0101); the Mission Connect Mild Traumatic Brain Injury Consortium, funded by the Department of Defense, W81XWH-08-2-0143; the Nanoscale Science and Engineering Initiative of the National Science Foundation under NSF Award EEC-0647452 for funding through the NSF Center for Biological and Environmental Nanotechnology; The University of Texas M. D. Anderson Cancer Center (UTMDACC) PANTHEON Program; NIH Cancer Center Support Grant CA16672; and UTMDACC Cancer Center Support Grant (CA016672).

REFERENCES AND NOTES

- Jemal, A.; Siegel, R.; Xu, J.; Ward, E. *Cancer Statistics, 2010*. *CA Cancer J. Clin.* **2010**, *60*, 277–300.
- Carvalho, A. L.; Nishimoto, I. N.; Califano, J. A.; Kowalski, L. P. Trends in Incidence and Prognosis for Head and Neck Cancer in the United States: a Site-Specific Analysis of the SEER Database. *Int. J. Cancer* **2005**, *114*, 806–816.
- Lango, M. N. Multimodal Treatment for Head and Neck Cancer. *Surg. Clin. North Am.* **2009**, *89*, 43–52, viii.
- Hamburg, M. A.; Collins, F. S. The Path to Personalized Medicine. *New Engl. J. Med.* **2010**, *363*, 301–304.
- Schilsky, R. L. Personalized Medicine in Oncology: the Future is Now. *Nat. Rev. Drug Discovery* **2010**, *9*, 363–366.
- Riehemann, K.; Schneider, S. W.; Luger, T. A.; Godin, B.; Ferrari, M.; Fuchs, H. Nanomedicine-Challenge and Perspectives. *Angew. Chem., Int. Ed.* **2009**, *48*, 872–897.
- Ferrari, M. Cancer Nanotechnology: Opportunities and Challenges. *Nat. Rev. Cancer* **2005**, *5*, 161–171.
- Service, R. F. Materials and Biology. Nanotechnology Takes Aim at Cancer. *Science* **2005**, *310*, 1132–1134.
- Sinha, R.; Kim, G. J.; Nie, S.; Shin, D. M. Nanotechnology in Cancer Therapeutics: Bioconjugated Nanoparticles for Drug Delivery. *Mol. Cancer Ther.* **2006**, *5*, 1909–1917.
- Peer, D.; Karp, J. M.; Hong, S.; Farokhzad, O. C.; Margalit, R.; Langer, R. Nanocarriers as an Emerging Platform for Cancer Therapy. *Nat. Nanotechnol.* **2007**, *2*, 751–760.
- Davis, M. E.; Chen, Z. G.; Shin, D. M. Nanoparticle Therapeutics: an Emerging Treatment Modality for Cancer. *Nat. Rev. Drug Discovery* **2008**, *7*, 771–782.
- Bonner, J. A.; Maihle, N. J.; Folven, B. R.; Christianson, T. J. H.; Spain, K. The Interaction of Epidermal Growth-Factor and Radiation in Human Head and Neck Squamous-Cell Carcinoma Cell-Lines with Vastly Different Radiosensitivities. *Int. J. Radiat. Oncol.* **1994**, *29*, 243–247.
- Huang, S. M.; Bock, J. M.; Harari, P. M. Epidermal Growth Factor Receptor Blockade with C225 Modulates Proliferation, Apoptosis, and Radiosensitivity in Squamous Cell Carcinomas of the Head and Neck. *Cancer Res.* **1999**, *59*, 1935–1940.
- Saleh, M. N.; Raisch, K. P.; Stackhouse, M. A.; Grizzle, W. E.; Bonner, J. A.; Mayo, M. S.; Kim, H. G.; Meredith, R. F.; Wheeler, R. H.; Buchsbaum, D. J. Combined Modality Therapy of A431 Human Epidermoid Cancer Using Anti-EGFR Antibody C225 and Radiation. *Cancer Biother. Radiopharm.* **1999**, *14*, 451–463.
- Vermorken, J. B.; Mesia, R.; Rivera, F.; Remenar, E.; Kawecki, A.; Rottey, S.; Erfan, J.; Zabolotnyy, D.; Kienzer, H. R.; Cupissol, D.; et al. Platinum-Based Chemotherapy Plus Cetuximab in Head and Neck Cancer. *New Engl. J. Med.* **2008**, *359*, 1116–1127.
- Bonner, J. A.; Harari, P. M.; Giralt, J.; Azarnia, N.; Shin, D. M.; Cohen, R. B.; Jones, C. U.; Sur, R.; Raben, D.; Jassem, J.; et al. Radiotherapy plus Cetuximab for Squamous-Cell Carcinoma of the Head and Neck. *New Engl. J. Med.* **2006**, *354*, 567–578.
- Rubin Grandis, J.; Melhem, M. F.; Gooding, W. E.; Day, R.; Holst, V. A.; Wagener, M. M.; Drenning, S. D.; Twardy, D. J. Levels of TGF- α and EGFR Protein in Head and Neck Squamous Cell Carcinoma and Patient Survival. *J. Natl. Cancer Inst.* **1998**, *90*, 824–832.
- Berlin, J. M.; Leonard, A. D.; Pham, T. T.; Sano, D.; Marcano, D. C.; Yan, S.; Fiorentino, S.; Milas, Z. L.; Kosynkin, D. V.; Price, B. K.; et al. Effective Drug Delivery, *In Vitro* and *In Vivo*, by Carbon-Based Nanovectors Noncovalently Loaded with Unmodified Paclitaxel. *ACS Nano* **2010**, *4*, 4621–4636.
- Chen, Z. Y.; Kobashi, K.; Rauwald, U.; Booker, R.; Fan, H.; Hwang, W. F.; Tour, J. M. Soluble Ultra-Short Single-Walled Carbon Nanotubes. *J. Am. Chem. Soc.* **2006**, *128*, 10568–10571.
- Price, B. K.; Lomeda, J. R.; Tour, J. M. Aggressively Oxidized Ultra-Short Single-Walled Carbon Nanotubes Having Oxidized Sidewalls. *Chem. Mater.* **2009**, *21*, 3917–3923.
- Stephenson, J. J.; Hudson, J. L.; Leonard, A. D.; Price, B. K.; Tour, J. M. Repetitive Functionalization of Water-Soluble Single-Walled Carbon Nanotubes. Addition of Acid-Sensitive Addends. *Chem. Mater.* **2007**, *19*, 3491–3498.
- Berlin, J. M.; Pham, T. T.; Sano, D.; Mohamedali, K. A.; Marcano, D. C.; Myers, J. N.; Tour, J. M. Noncovalent Functionalization of Carbon Nanovectors with an Antibody Enables Targeted Drug Delivery. *ACS Nano* **2011**, *5*, 6643–6650.
- Gupta, A. K.; McKenna, W. G.; Weber, C. N.; Feldman, M. D.; Goldsmith, J. D.; Mick, R.; Machtay, M.; Rosenthal, D. I.; Bakanauskas, V. J.; Cerniglia, G. J.; et al. Local Recurrence in Head and Neck Cancer: Relationship to Radiation Resistance and Signal Transduction. *Clin. Cancer Res.* **2002**, *8*, 885–892.
- Milas, L.; Mason, K.; Hunter, N.; Petersen, S.; Yamakawa, M.; Ang, K.; Mendelsohn, J.; Fan, Z. *In Vivo* Enhancement of Tumor Radioresponse by C225 Antiepidermal Growth Factor Receptor Antibody. *Clin. Cancer Res.* **2000**, *6*, 701–708.
- Sano, D.; Matsumoto, F.; Valdecana, D.; Zhao, M.; Molkentine, D. P.; Takahashi, Y.; Hanna, E. Y.; Papadimitrakopoulou, V. A.; Heymach, J. V.; Milas, L.; et al. Vandetanib Restores Head and Neck Squamous Cell Carcinoma Cells' Sensitivity to Cisplatin and Radiation *in Vivo* and *in Vitro*. *Clin. Cancer Res.* **2011**, *17*, 1815–1827.
- Milas, L.; Fujii, T.; Hunter, N.; Elshaikh, M.; Mason, K.; Plunkett, W.; Ang, K. K.; Hittelman, W. Enhancement of Tumor Radioresponse *in Vivo* by Gemcitabine. *Cancer Res.* **1999**, *59*, 107–114.
- Sawai, A.; Chandralapaty, S.; Greulich, H.; Gonen, M.; Ye, Q.; Artega, C. L.; Sellers, W.; Rosen, N.; Solit, D. B. Inhibition of

- Hsp90 Down-Regulates Mutant Epidermal Growth Factor Receptor (EGFR) Expression and Sensitizes EGFR Mutant Tumors to Paclitaxel. *Cancer Res.* **2008**, *68*, 589–596.
28. Zhou, G.; Xie, T. X.; Zhao, M.; Jasser, S. A.; Younes, M. N.; Sano, D.; Lin, J.; Kupferman, M. E.; Santillan, A. A.; Patel, V.; *et al.* Reciprocal Negative Regulation Between S100A7/Psoriasis and *Beta*-Catenin Signaling Plays an Important Role in Tumor Progression of Squamous Cell Carcinoma of Oral Cavity. *Oncogene* **2008**, *27*, 3527–3538.
29. Sano, D.; Choi, S.; Milas, Z. L.; Zhou, G.; Galer, C. E.; Su, Y. W.; Gule, M.; Zhao, M.; Zhu, Z.; Myers, J. N. The Effect of Combination Anti-Endothelial Growth Factor Receptor and Anti-Vascular Endothelial Growth Factor Receptor 2 Targeted Therapy on Lymph Node Metastasis: a Study in an Orthotopic Nude Mouse Model of Squamous Cell Carcinoma of the Oral Tongue. *Arch. Otolaryngol. Head Neck Surg.* **2009**, *135*, 411–420.
30. Myers, J. N.; Holsinger, F. C.; Jasser, S. A.; Bekele, B. N.; Fidler, I. J. An Orthotopic Nude Mouse Model of Oral Tongue Squamous Cell Carcinoma. *Clin. Cancer Res.* **2002**, *8*, 293–298.
31. Choi, H. S.; Liu, W.; Liu, F.; Nasr, K.; Misra, P.; Bawendi, M. G.; Frangioni, J. V. Design Considerations for Tumour-Targeted Nanoparticles. *Nat. Nanotechnol.* **2010**, *5*, 42–47.